

# Ultra-Compact Silicon Mode Converter Based on a Zigzag-type Metasurface Structure

Hongwei Wang, Yu He, Lu Sun, Yong Zhang, and Yikai Su\*

State Key Lab of Advanced Optical Communication Systems and Networks, Department of Electronic Engineering,  
Shanghai Jiao Tong University, Shanghai 200240, China  
Author e-mail address: yikaisu@sjtu.edu.cn

**Abstract:** An ultra-compact silicon waveguide mode converter is proposed and experimentally demonstrated using an all-dielectric metasurface structure with zigzag-type periodic perturbations.  
© 2021 The Author(s)

## 1. Introduction

On-chip silicon mode division multiplexing (MDM) technology is a promising solution for high-capacity integration, which exhibits compact footprint and compatibility with complementary metal oxide semiconductor (CMOS) fabrication [1,2]. A mode converter, which is capable of converting one selected waveguide mode to another, is one of the key components in MDM systems. Recently, many silicon on-chip mode converters were proposed based on phase matching [3], coherent scattering [4], and beam shaping [5]. However, these devices may face the challenges of large footprints, limited operation bandwidths and relatively high insertion losses. Several waveguide-based mode converters were realized based on the phase-gradient metasurfaces [6], periodic perturbed nanoscale waveguides [7] and tilted sub-wavelength periodic perturbation structures [8]. It is highly desired to further shrink the device footprint and realize a high-order waveguide mode converter.

In this paper, we propose and experimentally demonstrate an ultra-compact mode converter based on an all-dielectric metasurface structure. By introducing a zigzag-type periodic perturbation, the distribution of the mode coupling coefficients along the propagation direction can be manipulated, thus a high-efficient mode conversion can be achieved with a compact footprint. As a proof-of-concept experiment, two silicon waveguide mode converters are demonstrated, which can convert the TE<sub>0</sub> mode to TE<sub>1</sub> and TE<sub>2</sub> modes, respectively. The device lengths are 3.71 μm and 3.45 μm for the TE<sub>0</sub>-to-TE<sub>1</sub> and TE<sub>0</sub>-to-TE<sub>2</sub> waveguide mode converters, respectively. The insertion losses are lower than 1 dB and the crosstalk values are below -10 dB in a wavelength range of 30 nm and 20 nm for the TE<sub>0</sub>-to-TE<sub>1</sub> and TE<sub>0</sub>-to-TE<sub>2</sub> mode converters, respectively. Our proposed mode converter has the potential to be scaled to realize an arbitrary high-order mode conversion. For example, the simulated conversion efficiencies for the TE<sub>0</sub>-to-TE<sub>9</sub> and TE<sub>0</sub>-to-TE<sub>12</sub> mode converters are 74.5% and 73%, respectively.

## 2. Device design and simulation

The 3D view of the proposed waveguide mode converter is shown in Fig. 1(a). Dielectric metasurface structure is introduced to assist the mode conversion. By adopting a zigzag-type sub-wavelength periodic perturbation, the overlap of the mode profiles between two waveguide modes can be increased, thus a high-efficient mode conversion can be achieved. According to the coupled mode theory, the conversion between two waveguide modes is described by the following equations [9]:

$$-\frac{\partial A}{\partial z} = j\kappa_{ab} B e^{j(\beta_a - \beta_b)z}, \quad -\frac{\partial B}{\partial z} = j\kappa_{ba} A e^{-j(\beta_a - \beta_b)z}, \quad (1)$$

where  $A$  and  $B$  are the amplitudes of waveguide modes  $a$  and  $b$ , respectively.  $\kappa_{ab}$  and  $\kappa_{ba}$ , which are related to the periodic perturbation  $\Delta\epsilon(x, y, z)$ , represent the exchange coupling coefficients between modes  $a$  and  $b$ . Based on Eq. (1), the phase matching condition for the mode conversion between mode  $a$  and mode  $b$  is [9]

$$\delta = \frac{2\pi}{\sqrt{(\beta_a - \beta_b)^2 + 4\kappa_{ab}^2}}, \quad (2)$$

where  $\delta$  is the period of the  $\Delta\epsilon(x, y, z)$ . In this work, a zigzag-type metasurface structure is utilized. Sharp turns are placed by referring to the electric field distributions of the target modes, as shown in Figs. 2(a-d), to maximize the overlapping between the input mode and the target mode. Here, we take the coupling process of the TE<sub>0</sub>-to-TE<sub>2</sub> converter as an example. As shown in Fig. 1(b), the TE<sub>0</sub> mode is gradually converted to the TE<sub>2</sub> mode with  $\kappa_{02}$  changing as a sinusoidal function along the propagation direction. After propagating over  $\delta/2$ , the TE<sub>0</sub> mode and the

TE<sub>2</sub> mode will be out of phase. Thus, it is necessary to change  $\kappa_{02}$  from a negative value to a positive value to ensure that the TE<sub>0</sub> mode can always constructively facilitate the conversion to the target mode.

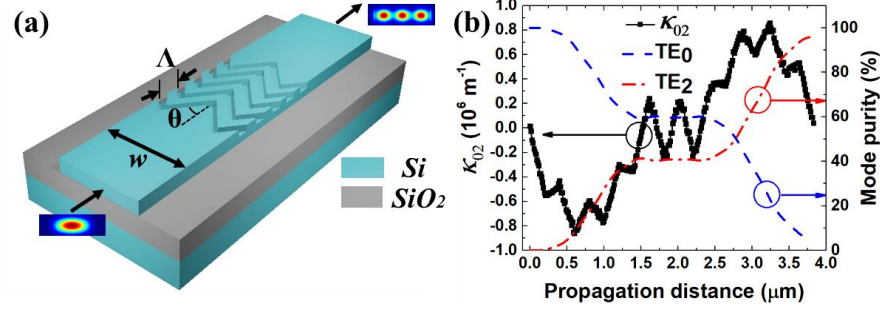


Fig. 1. (a) Schematic configuration for the proposed waveguide mode converter. (b) Calculated mode coupling coefficient ( $\kappa_{ab}$ ) between waveguide modes TE<sub>0</sub> and TE<sub>2</sub> (black thick curve), and the mode purity curves of the TE<sub>0</sub> mode (red dashed) and TE<sub>2</sub> mode (blue thin) as a function of propagation distance.

By properly designing the structure of the periodical perturbation, the maximum value of  $\kappa_{0j}$  can be obtained, which leads to an ultra-compact footprint. The coupling length is  $L = \delta + n \Lambda$  and the angle of the parallelogram can be calculated as  $\theta = \arctan[w/((j+1)\delta)]$ . The number of sharp angles ( $\alpha$ ) and the order of the transformed mode ( $j$ ) satisfy  $\alpha = j+1$ . For the TE<sub>0</sub>-to-TE<sub>1</sub> and TE<sub>0</sub>-to-TE<sub>2</sub> mode converters, the theoretical results of  $\theta$  are 17.8° and 18.75° with  $\delta = 2.747 \mu\text{m}$  and  $\delta = 2.838 \mu\text{m}$ , respectively.

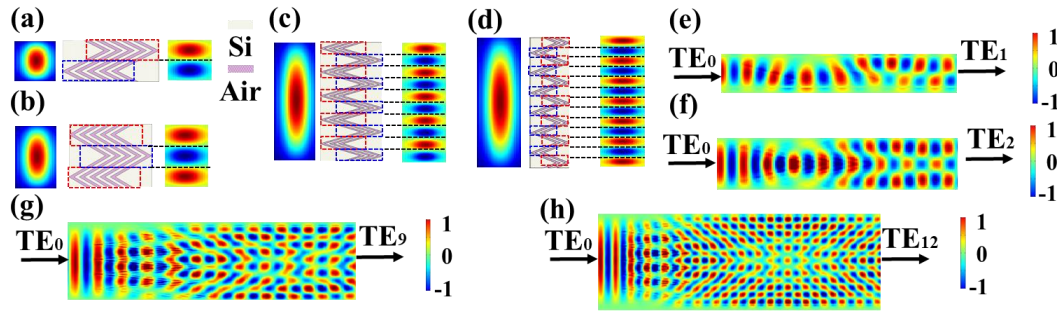


Fig. 2. (a-d) Top view of schematic configuration, (e-h) simulated electric field ( $E_y$ ) distribution for the proposed TE<sub>0</sub>-to-TE<sub>1</sub>, TE<sub>0</sub>-to-TE<sub>2</sub>, TE<sub>0</sub>-to-TE<sub>9</sub> and TE<sub>0</sub>-to-TE<sub>12</sub> mode converters, respectively.

Figs. 2(a-d) show the top view of the schematic of the proposed TE<sub>0</sub>-to-TE<sub>1</sub>, TE<sub>0</sub>-to-TE<sub>2</sub>, TE<sub>0</sub>-to-TE<sub>9</sub> and TE<sub>0</sub>-to-TE<sub>12</sub> mode converters. Detailed design parameters of mode converters are provided in Table 1. Figs. 2(e-h) show the top view of simulated electric field ( $E_y$ ) distribution of the proposed three mode converters. The simulated mode purity of the four mode converters are 76%, 84.2%, 74.5% and 73% at  $\lambda = 1550 \text{ nm}$ , respectively.

Table 1. Detailed design parameters of the mode converters

Mode converter	Width ( $\mu\text{m}$ )	Period (nm)	Duty	$n$	$\theta$ ( $^\circ$ )	Etching depth	Length ( $\mu\text{m}$ )
TE <sub>0</sub> -to-TE <sub>1</sub>	1.1	400	75%	5	20	120	3.71
TE <sub>0</sub> -to-TE <sub>2</sub>	1.8	400	50%	5	20	120	3.45
TE <sub>0</sub> -to-TE <sub>9</sub>	5	400	50%	3	16	120	2.98
TE <sub>0</sub> -to-TE <sub>12</sub>	6.24	400	50%	2	16	120	2.56

### 3. Device fabrication and measurement results

Multiple devices were fabricated on a SOI platform with a 220-nm-thick silicon on top of a 3- $\mu\text{m}$  SiO<sub>2</sub> buried oxide. Grating couplers, silicon waveguides and metasurface structures were patterned using electron beam lithography (Vistec EBPG-5200<sup>+</sup>) and etched by 70nm, 220nm and 120nm, respectively, through inductively coupled plasma (ICP) etching. The scanning electron microscope (SEM) photos and optical microscope photos of the fabricated TE<sub>0</sub>-to-TE<sub>1</sub> and TE<sub>0</sub>-to-TE<sub>2</sub> mode converters are shown in Figs. 3(a-d), respectively.

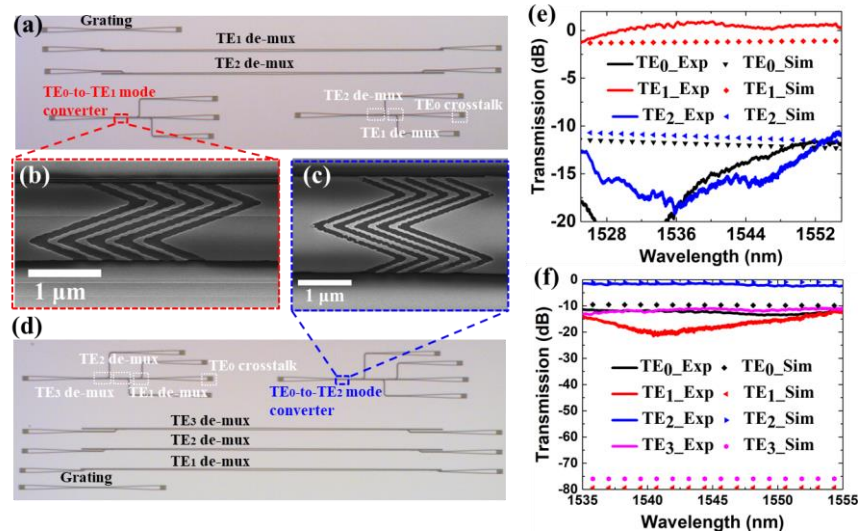


Fig. 3a and 3d show the optical microscope photos of the fabricated TE<sub>0</sub>-to-TE<sub>1</sub> and TE<sub>0</sub>-to-TE<sub>2</sub> mode converters, respectively. Fig. 3b and 3c are the SEM photos of the fabricated TE<sub>0</sub>-to-TE<sub>1</sub> and TE<sub>0</sub>-to-TE<sub>2</sub> mode converters, respectively. Simulated and experimental transmission results of the Fig. 3e: TE<sub>0</sub>-to-TE<sub>1</sub> mode converter and Fig. 3 (f): TE<sub>0</sub>-to-TE<sub>2</sub> mode converter.

Mode de-multiplexers based on asymmetrical directional couplers are cascaded after the mode converters to recover the output high-order mode signals to TE<sub>0</sub> modes for the measurements. The measured insertion losses of the fabricated mode de-multiplexers for TE<sub>1</sub>, TE<sub>2</sub>, TE<sub>3</sub> de-multiplexing are 9.7 dB, 7.4 dB, and 8 dB at  $\lambda = 1550$  nm, respectively. The measured transmission responses of the fabricated TE<sub>0</sub>-to-TE<sub>1</sub> and TE<sub>0</sub>-to-TE<sub>2</sub> mode converters are shown in Figs. 3(e) and (f), respectively. The transmission spectra were normalized to that of the grating couplers or mode de-multiplexers fabricated on the same wafer. For the TE<sub>0</sub>-to-TE<sub>1</sub> mode converter, the conversion loss is lower than 1 dB and the crosstalk value is below -10 dB in the wavelength range of 1525 nm ~ 1555 nm. For the TE<sub>0</sub>-to-TE<sub>2</sub> mode converter, the conversion loss is < 1 dB and the crosstalk value is < -10 dB in the wavelength range of 1535 nm ~ 1555 nm. The dashed curves in Figs. 3(e) and (f) show the simulated responses of the mode converters. The discrepancy between the experimental and simulation results can be mainly attributed to the deviations of the etching depth caused by fabrication imperfections.

#### 4. Conclusion and discussion

We have proposed and experimentally demonstrated a compact silicon waveguide mode converter implemented with all-dielectric metasurface structure. The device lengths are 3.71  $\mu\text{m}$  and 3.45  $\mu\text{m}$  for the TE<sub>0</sub>-to-TE<sub>1</sub> and TE<sub>0</sub>-to-TE<sub>2</sub> mode converters, respectively. The conversion losses are lower than 1 dB, and the crosstalk values are below -10 dB in the wavelength range of 1525 nm ~ 1555 nm and 1535 nm ~ 1555 nm, respectively. Our proposed waveguide mode converter can also be scaled to realize higher-order waveguide mode conversions.

#### 5. References

- [1] R. Soref, "Mid-infrared photonics in silicon and germanium," *Nat. Photonics* **4**, 495 (2010).
- [2] Y. Su, Y. Zhang, C. Qiu, X. Guo, and L. Sun, "Silicon photonic platform for passive waveguide devices: materials, fabrication, and applications," *Adv. Mater. Technol.* 1-19, 1901153 (2020).
- [3] D. X. Dai, J. Wang, Y. C. Shi, "Silicon mode (de)multiplexer enabling high capacity photonic networks-on-chip with a single-wavelength-carrier light," *Opt. Lett.* **38**, 1422 (2013).
- [4] V. Liu, D. A. B. Miller, S. H. Fan, "Ultra-compact photonic crystal waveguide spatial mode converter and its connection to the optical diode effect," *Opt. Express* **20**, 28388 (2012).
- [5] B. T. Lee, S. Y. Shin, "Mode-order converter in a multimode waveguide," *Opt. Lett.* **28**, 1660 (2003).
- [6] Z. Y. Li, M. H. Kim, C. Wang, Z. H. Han, S. Shrestha, A. C. Overvig, M. Lu, A. Stein, A. M. Agarwal, M. Loncar, N. F. Yu, "Controlling propagation and coupling of waveguide modes using phase-gradient metasurfaces," *Nat. Nanotechnol.* **12**, 675 (2017).
- [7] D. Ohana, B. Desiatov, N. Mazurski, U. Levy, "Dielectric metasurface as a platform for spatial mode conversion in nanoscale waveguides," *Nano. Lett.* **16**, 7956 (2016).
- [8] H. Wang, Y. Zhang, Y. He, Q. Zhu, L. Sun and Y. Su, "Compact silicon waveguide mode converter employing dielectric metasurface structure," *Adv. Opt. Mater.* **7**, 4, 1801191 (2019).
- [9] L. W. Luo, N. Ophir, C. P. Chen, L. H. Gabrielli, C. B. Poitras, K. Bergmen, M. Lipson, "WDM-compatible mode-division multiplexing on a silicon chip," *Nat. Commun.* **5** (2014).